Ferromagnetic Domain Structures and Nanoclusters in $Nd_{1/2}Sr_{1/2}MnO_3$

T. Asaka,[1,2] Y. Anan,[1] T. Nagai,[1] S. Tsutsumi,[2] H. Kuwahara,[3] K. Kimoto,[1] Y. Tokura,[4,5] and Y. Matsui[1]

[1]*Advanced Materials Laboratory (AML), National Institute for Materials Science (NIMS), Tsukuba 305-0044, Japan*

[2]*School of Education, Waseda University, Tokyo 169-8085, Japan*

[3]*Department of Physics, Sophia University, Tokyo 102-8554, Japan*

[4]*Correlated Electron Research Center (CERC), National Institute of Advanced Industrial Science and Technology (AIST), Tsukuba 305-0046, Japan*

[5]*Department of Applied Physics, University of Tokyo, Tokyo 113-8656, Japan*

(Received 22 April 2002; published 23 October 2002)

Magnetic domain structures of $Nd_{1/2}Sr_{1/2}MnO_3$ were investigated by means of low-temperature Lorentz electron microscopy. On cooling, magnetic domain walls started to appear at 250 K, and they were oriented straight along the [100] and [110] directions. With a further decrease in temperature, the volume of each magnetic domain increased with discontinuous domain-wall jumps. A characteristic granular image was observed at around 140 K, near the charge-ordering transition temperature. We consider that this originated from ferromagnetic nanoclusters that appeared in the antiferromagnetic matrix.

DOI: 10.1103/PhysRevLett.89.207203 PACS numbers: 75.70.Kw, 71.30.+h, 75.30.Kz, 75.50.Dd

Manganese oxides with distorted perovskite structures have been attracting a lot of attention because of their unusual electron-transport and magnetic properties, such as colossal magnetoresistance (CMR) and charge-ordering phenomena. It is known that the CMR property and melting transitions in the charge-ordering phase are closely related to the appearance of a ferromagnetic metallic state. Usually, the ferromagnetic metallic state in manganese oxides is described in terms of the double-exchange (DE) mechanism [1]. On the other hand, magnetic domains and domain walls in manganese oxides in the ferromagnetic phase may strongly affect not only the magnetic properties but also the electron-transport properties of these oxides. Recently, Mathur *et al.* reported that the measured resistivity of a magnetic domain wall is considerably higher, by several orders of magnitude, than that expected due to the simple DE mechanism [2]. The scattering of charge carriers by domain walls may be a possible cause of low-temperature magnetoresistance [3]. In relation to the CMR property, moreover, many researchers have stated the existence of ferromagnetic microclusters and minority ferromagnetic phases in manganese oxides [4,5]. The existence of such ferromagnetic microclusters may give rise to low-field magnetoresistance by tunneling, as the intergrain-tunneling phenomenon observed in the polycrystalline granular structure of manganese oxides [6,7].

Magnetic domains in perovskite-type manganese oxides and their related materials have been directly observed by using various techniques, such as magnetic force microscopy [8], scanning Hall probe microscopy [9], and Kerr microscopy [6]. Recently, Lloyd *et al.* have investigated magnetic domain walls in ferromagnetic $La_{0.7}Ca_{0.3}MnO_3$ films by using the Fresnel method in Lorentz transmission electron microscopy (TEM) [10]. There are two commonly used imaging methods, called the Fresnel and the Foucault methods, in Lorentz TEM [11]. The Fresnel method enables observing domain walls rather than domains. In this study, we mainly used the Fresnel method. Lorentz TEM is characterized by high resolution on the nanometer scale and high sensitivity even to small variations in magnetization. Using the Fresnel method of Lorentz TEM, we can directly observe the interaction between domain walls and lattice defects and the dynamic behavior of domain walls in real time.

We focused on $Nd_{1/2}Sr_{1/2}MnO_3$ with orthorhombically distorted perovskite structure. This compound exhibits phase transitions at low temperatures. On cooling, $Nd_{1/2}Sr_{1/2}MnO_3$ undergoes the following transitions [12]: from the paramagnetic insulator state to the ferromagnetic metal state at the Curie temperature, $T_C \sim 250$ K, and then to the charge-ordered CE-type antiferromagnetic state at the charge-ordering temperature, $T_{CO} \sim 150$ K. It is known that the ferromagnetic (FM) metal—charge-ordered (CO) antiferromagnetic insulator phase transition is a first-order one [12], accompanying with the *I*bmm orthorhombic (FM)—$P2_1/m$ monoclinic (CO) structural phase transition [13].

In this paper, we investigate $Nd_{1/2}Sr_{1/2}MnO_3$ at low temperatures by using Lorentz TEM. The behavior of magnetic domain structures and the relationship between crystal structures and the magnetic domain structures is discussed in detail. Furthermore, we describe characteristic granular contrast observed at temperatures close to T_{CO}, only in heating. Its origin is discussed in terms of the appearance of ferromagnetic nanoclusters. To the best of our knowledge, our findings provide the first direct evidence of the spontaneous generation of ferromagnetic nanoclusters in manganese oxides.

Single crystalline samples of $Nd_{1/2}Sr_{1/2}MnO_3$ were grown by using a floating-zone method. (The crystal growth details are described elsewhere [14].) The

obtained crystals had a multidomain crystallographic structure with a common fourfold axis in the pseudocubic structure. For the observation using Lorentz TEM, the samples were thinned by Ar^+ ion sputtering. The specimens were examined using a field-emission gun Lorentz electron microscope (Hitachi HF-3000L) operating at 300 kV. Because the T_C of this compound is ~250 K, the specimens were cooled from room temperature to 80 K in an Oxford liquid nitrogen cooling holder in order to observe the domain walls. Here, we briefly describe the principle of imaging in the Fresnel method of Lorentz TEM [11]. When the incident electron beam penetrates a specimen with a magnetic domain structure, the electrons are deflected by the Lorentz force. If the objective lens of the Lorentz electron microscope is underfocused or overfocused, electrons coming through different domains will produce images in which the walls appear as bright (white) and dark (black) lines. These lines reverse their contrast between the underfocused and overfocused images. The bright (white) and dark (black) lines corresponding to the domain walls are called convergent images and divergent images, respectively. These images disappear under in-focus conditions.

We show the images of magnetic domain walls of $Nd_{1/2}Sr_{1/2}MnO_3$ in the ferromagnetic state. Figures 1(a)–1(c) show the typical Lorentz TEM images of the present compound observed at ~225 K, taken with the underfocus of −500 μm, in-focus condition, and the overfocus of +500 μm, respectively. Characteristic straight black lines and white lines can be seen in Figs. 1(a) and 1(c), but they almost disappear in Fig. 1(b). The black lines and white lines in Fig. 1(a) reverse their contrast in Fig. 1(c). We concluded from such observation that the straight black lines and white lines represent, respectively, divergent and convergent images of the magnetic domain walls. We found that the manganese oxides had a magnetic domain structure, similar to the one of typical ferromagnetic metal materials, such as Fe and Co [11]. The curved lines in each image, on the other hand, show bend contours and thickness fringes, which are not due to the magnetism. The straight lines indicated by the arrows in the center of Fig. 1(b) are due to twin boundaries between which microtwins formed with crystallographic axes rotated 90° on the c axis. We can see convergent and divergent images at the twin boundaries in Figs. 1(a) and 1(c). Therefore, we can conclude that the twin boundaries play the role of magnetic domain walls at temperatures between 150 and 245 K. This indicates that magnetic domain wall is pinned strongly at the structural twin boundaries.

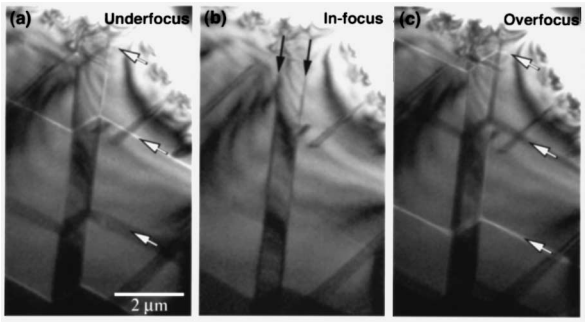

FIG. 1. Lorentz TEM images of $Nd_{1/2}Sr_{1/2}MnO_3$ at ~225 K: (a) underfocused, (b) in focus, and (c) overfocused. Straight black lines and white lines indicated by white arrows in (a) and (c) represent, respectively, divergent and convergent images of domain walls. Arrows in (b) show the twin boundaries.

Figure 2 shows a Lorentz TEM image of the ab plane in $Nd_{1/2}Sr_{1/2}MnO_3$ at 180 K. The domain walls were oriented along the [100] direction in the main part, and along the [110] direction in the microtwins. We examined the domains by electron diffraction and found from the magnetic splitting of the central spot in the diffraction pattern that the direction of magnetization in each domain was along the long sides of the domain, as indicated by the white arrows in Fig. 2. This suggests that the compound has a magnetocrystalline anisotropy. We consider that the easy directions of magnetization are the [100] and [110] directions.

Figure 3 shows the dynamic behavior of magnetic domain walls on the changing in temperature. On cooling, magnetic domain walls started to appear at 245 K (near T_C). They were first observed inside the microtwins as shown in Fig. 3(b). As the temperature decreased, while the bulk magnetization in the present compound increased according to the measurements of magnetic susceptibility, the volume of ferromagnetic phase increased gradually, as shown in Figs. 3(b)–3(d). The movements of the domain walls can be characterized as discontinuous domain-wall jumps. This suggests that the domain walls got released from the pinning sites as a result of thermal excitation, and then jumped to new stable positions [15]. Such discontinuous domain-wall

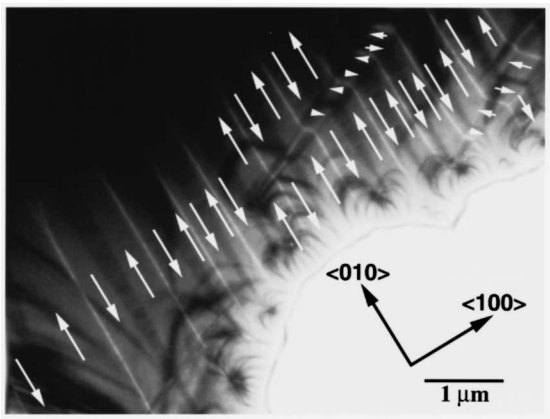

FIG. 2. A [001]-zone Lorentz TEM image obtained at 180 K. Magnetic domain walls are oriented along the [100] and [110] directions. White arrows indicate the direction of magnetization within each domain.

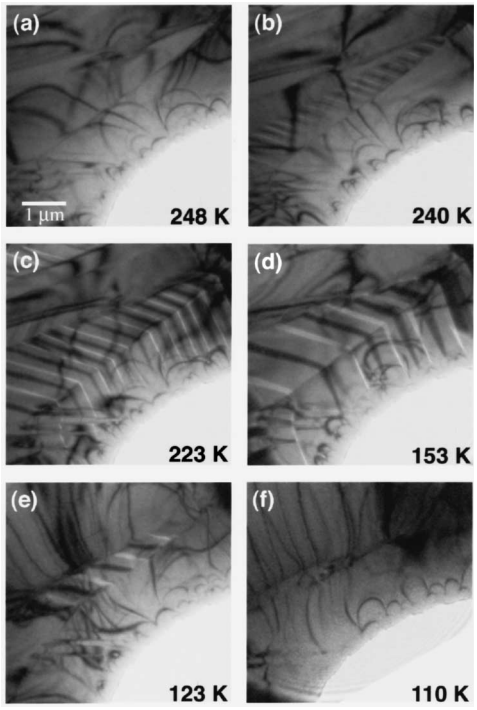

FIG. 3. Lorentz TEM images of magnetic domain walls obtained at (a) 248, (b) 240, (c) 223, (d) 153, (e) 123, and (f) 110 K, during the cooling process.

jumps activated by thermal excitation and the ac field in the manganese oxides, which were observed by means of ac susceptibility measurements, have already been reported [16]. Here, some of the domain walls were always located at the twin boundaries, as mentioned above. Therefore, the twin boundaries can be regarded as a strong pinning site. When the temperature decreased below 150 K, the ferromagnetic phase characterized by the presence of domain walls gradually disappeared (near T_{CO}) due to the growth of the antiferromagnetic charge-ordering phase, as shown in Figs. 4(e) and 4(f).

We also examined in the heating process from 80 K and obtained the Lorentz TEM images, similar to the ones at respective temperatures in the cooling process, except for the following magnetic structure at T_{CO}. Figure 4(a) shows a Lorentz TEM image of $Nd_{1/2}Sr_{1/2}MnO_3$ at 80 K. No characteristic magnetic contrast was observed because the present compound enters an antiferromagnetic charge/orbital-ordered state below T_{CO}. We verified that the compound was in the charge/orbital-ordered state by means of electron diffraction and dark-field imaging. On heating from 80 K, characteristic granular contrast, that was formed with 30–40 nm in diameter, was observed in the whole area at around 140 K, a temperature close to T_{CO}, as shown in Fig. 4(b). Here, no dynamic behavior such as movements of small "particles" was observed in the granular images. These granular structures disappeared rapidly at ~145 K [Fig. 4(c)] and ferromagnetic domain walls started to appear at ~155 K, as

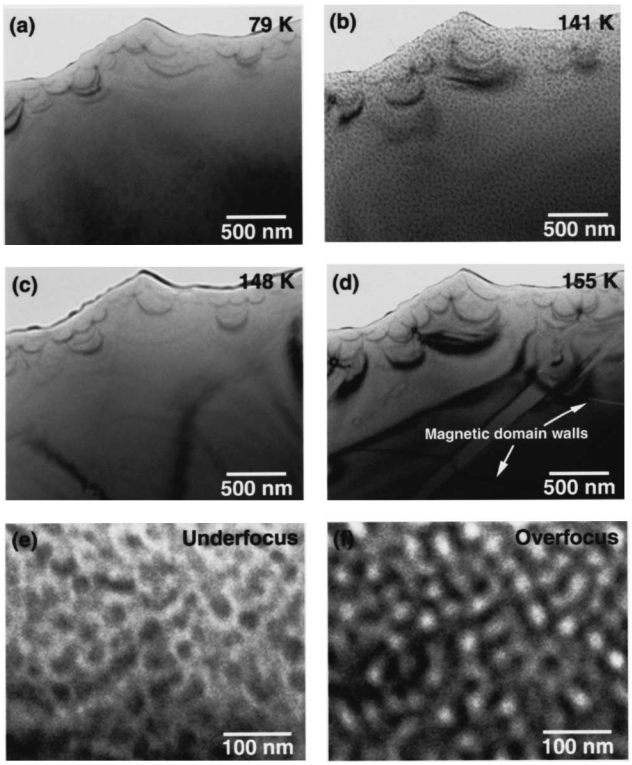

FIG. 4. Lorentz TEM images obtained at (a) 79, (b) 141, (c) 148, and (d) 155 K during the heating process, and high-magnification images of the granular structure obtained in (e) the underfocused condition and (f) the overfocused condition, respectively.

shown in Fig. 4(d). No granular contrast was observed in the cooling process.

Here, we discuss the origin of the granular structure. Figures 4(e) and 4(f) show enlarged granular images obtained in the underfocused condition and the overfocused condition, respectively. The granular contrast disappeared under the in-focus condition. The contrast in these images is due to the random spatial distribution of the objects that lead to the difference in the phase of the electron waves scattered through the specimen. The granular contrast appeared only at temperatures close to T_{CO}, as mentioned above. We inferred from this that the contrast is due to the distribution of the magnetic objects and/or the related effect induced by the magnetic and structural phase transition (e.g., the local strains). The magnetic objects give rise to the change in the phase of the electron waves. We consider that the origin of the granular contrast is the random distribution of ferromagnetic nanoclusters in the antiferromagnetic matrix. Here, this compound is in the insulating phase at ~140 K; that is, the ferromagnetic nanoclusters cannot contribute to bulk electronic conduction. This could be caused by a lack of percolative electronic conduction [17] and the scattering of charge carriers by the interfaces between the ferromagnetic nanoclusters and the antiferromagnetic matrix.

We also consider that this granular state is a result of spontaneous clustering of spins. This spontaneous granular state is a nucleation stage in the first-order phase transition in the present system. A magnetic granular state is usually observed in materials consisting of magnetic fine particles of the nanometer size and immiscible and nonmagnetic matrices with unique properties such as giant magnetoresistivity due to tunneling [18] and a soft magnetic property [19]. The Lorentz images of such magnetic granular materials [20] are similar to the granular images in Figs. 4(b), 4(e), and 4(f). In the present manganese oxides, the granular state appeared spontaneously with no artificial nanotexture. Moreover, recently, characteristic granular superconductivity has been observed in underdoped high-T_C superconductors, which is a result of tunneling between hole-rich superconducting nanodomains [21]. The appearance of the granular state of nanoclusters in the strongly correlated electron system may be an intrinsic and characteristic phenomenon, which would be associated with the electronic phase separation [17,22].

The authors thank Professor S. Mori (Osaka Prefecture University), Professor T. Arima (University of Tsukuba), Dr. T. Kimura (University of Tokyo), and Dr. Y. Tomioka (CERC) for their valuable discussions. We also thank C. Tsuruta (AML-NIMS) for his collaborations.

[1] C. Zener, Phys. Rev. **82**, 403 (1951); P.W. Anderson and H. Hasegawa, Phys. Rev. **100**, 675 (1955).
[2] N. D. Mathur *et al.*, J. Appl. Phys. **86**, 6287 (1999).
[3] P. Schiffer *et al.*, Phys. Rev. Lett. **75**, 3336 (1995); M. Yamanaka and N. Nagaosa, J. Phys. Soc. Jpn. **65**, 3088 (1996); G. Tatara and H. Fukuyama, Phys. Rev. Lett. **78**, 3773 (1997).
[4] J. M. De Teresa *et al.*, Nature (London) **386**, 256 (1997); O. Chauvet *et al.*, Phys. Rev. Lett. **81**, 1102 (1998).
[5] M. Savosta *et al.*, Phys. Rev. B **62**, 545 (2000); M. M. Savosta and P. Novak, Phys. Rev. Lett. **87**, 137204 (2001).
[6] A. Gupta *et al.*, Phys. Rev. B **54**, 15629 (1996).
[7] H. Y. Hwang *et al.*, Phys. Rev. Lett. **77**, 2041 (1996).
[8] Q. Lu, C. C. Chen, and A. de Lozanne, Science **276**, 2006 (1997); Y. Wu *et al.*, Appl. Phys. Lett. **75**, 2295 (1999).
[9] T. Fukumura *et al.*, Science **284**, 1969 (1999).
[10] S. J. Lloyd *et al.*, Phys. Rev. B **64**, 172407 (2001).
[11] P. J. Grundy and R. S. Tebble, Adv. Phys. **17**, 153 (1968); P. B. Hirsh *et al.*, *Electron Microscopy of Thin Crystals* (Krieger, Malabar, Florida, 1977).
[12] H. Kuwahara *et al.*, Science **270**, 961 (1995).
[13] V. Caignaert *et al.*, Solid State Commun. **99**, 173 (1996); C. Ritter *et al.*, Phys. Rev. B **61**, R9229 (2000).
[14] H. Kuwahara *et al.*, Phys. Rev. B **56**, 9386 (1997).
[15] D. C. Jiles and D. L. Atherton, J. Magn. Magn. Mater. **61**, 48 (1986); J. Horvat *et al.*, J. Magn. Magn. Mater. **87**, 339 (1990).
[16] X. L. Wang *et al.*, Phys. Rev. B **58**, 2434 (1998); M. Muroi *et al.*, Phys. Rev. B **64**, 024423 (2001).
[17] M. Uehara *et al.*, Nature (London) **399**, 560 (1999); S.-W. Cheong *et al.*, Physica (Amsterdam) **318B**, 39 (2002).
[18] A. E. Berkowitz *et al.*, Phys. Rev. Lett. **68**, 3745 (1992); J. Q. Xiao, J. S. Jiang, and C. L. Chien, Phys. Rev. Lett. **68**, 3749 (1992).
[19] S. Ohnuma *et al.*, J. Appl. Phys. **79**, 5130 (1996).
[20] T. Tanji *et al.*, Phys. Rev. Lett. **83**, 1038 (1999); N. Aoyama *et al.*, Jpn. J. Appl. Phys. **39**, 5340 (2000).
[21] K. M. Lang *et al.*, Nature (London) **415**, 412 (2002).
[22] V. J. Emery and S. A. Kivelson, Physica (Amsterdam) **209C**, 597 (1993).